Journal of Applied Electrochemistry (2006) 36:1099–1104
DOI 10.1007/s10800-006-9191-2

Binder effect on cycling performance of silicon/carbon composite anodes for lithium ion batteries

LIBAO CHEN[1,2], XIAOHUA XIE[1,2], JINGYING XIE[1,2,*], KE WANG[1] and JUN YANG[3]
[1]*Energy Science and Technology Laboratory, Shanghai Institute of Microsystem and Information Technology, Chinese Academy of Sciences, Shanghai, 200050, China*
[2]*Graduate school of Chinese Academy of Sciences, Beijing, 100049, China*
[3]*Department of Chemical Engineering, Shanghai Jiao Tong University, Shanghai, 200240, China*
*(*author for correspondence, e-mail: jyxie@mail.sim.ac.cn)*

Received 13 October 2005; accepted in revised form 9 June 2006

Key words: acrylic adhesive, anode, binder, cycling performance, lithium ion batteries, silicon/carbon composite

Abstract

The cycling performance of a silicon/carbon composite anode has been significantly enhanced by using acrylic adhesive and modified acrylic adhesive as binder to fabricate the electrodes for lithium ion batteries. The capacity retentions of Si/C composite electrodes bound by acrylic adhesive and modified acrylic adhesive are 79% and 90% after 50 cycles, respectively. These two binders are electrochemically stable in the organic electrolyte in the working window. They also show larger adhesion strength between the coating and the Cu current collector as well as smaller solvent absorption in the electrolyte solvent than polyvinylidene fluoride (PVDF). Furthermore, sodium carboxyl methyl cellulose (CMC) plays an important role on improving the properties of acrylic adhesive, which increases the adhesive strength of acrylic adhesive and improves the activation of the electrodes.

1. Introduction

Currently, graphite is commercially used as the anode materials for lithium ion batteries. But, its discharging capacity is unlikely to increase much further due to its lower theoretical capacity of 372 mA h g^{-1} [1, 2]. Therefore, the development of a new generation of lithium ion batteries requires new anode materials with high lithium storage capacity and long life. In recent studies, silicon has been studied extensively as anode material due to its largest theoretic specific capacity of 4200 mA h g^{-1} [3–7]. However, this material exhibits a dramatic volume expansion and contraction during lithiation and delithiation. Such a morphological change can cause the pulverization of silicon particles and loss of contact between the silicon and the current collector, resulting in very poor cycling performance. To improve the cycling stability of silicon, three kinds of Si-based materials have been widely investigated. (i) Si-based composites. Nano- or submicro-silicon particles are dispersed in an active or inactive matrix to buffer the volume change of silicon particles, such as Si–C composite [8, 9], Si–Ag composite [10], Si–TiB_2 composite [11], and so on. Since the size of silicon particles are quite small, the volume change can be partially suppressed by the matrix. (ii) Silicon alloys. Silicon alloys such as Mg_2Si [12], NiSi and FeSi [13] have better cycling performance than silicon because of their lower volume change. (iii) Amorphous silicon materials. Amorphous materials can alleviate the inhomogeneous expansion caused by the insertion of lithium ions, which would occur in the crystalline materials [14–16].

Though aforesaid Si-based materials have demonstrated some beneficial effects on the cycling performance, they have shown very limited success on long cycling performance owing to the inevitable volume change from Si. Capacity fading is still problematic for meeting the requirement of practical applications. As is known, when the particles of electrodes expand/contract during lithiation/delithiation, large interparticle motion occurs, which may result in binder bonds being broken unless the polymer binder is highly extensible and reversible. Obviously, the binder may also play a very important role in stabilizing the electrode materials, especially for those with large volume change like silicon-based materials. Chen et al. [17] improved the cycling performance of $Si_{0.64}Sn_{0.36}$ alloy by using elastomeric PVDF-TFE-P binder to fabricate electrodes. Liu et al. [18] also enhanced the cycling life of the Si-based electrodes by using a modified elastomeric binder (mixture of SBR and CMC).

In this work, we prepared a type of Si/C composite in which nanosized silicon and fine graphite particle were homogeneously embedded in PVC pyrolyzed carbon

[19]. This material exhibited a better cycling performance than Si because the carbon matrix can partly buffer the volume change from Si. However, only PVC pyrolyzed carbon can hardly tolerate the volume change from Si upon long cycles. The Si/C composite particles could be cracked by the mechanical stress resulting from the volume changes from Si after some cycles [20]. Therefore, we used acrylic adhesive to further enhance the cycling performance of Si/C composite.

2. Experimental

2.1. *Si/C composite preparation*

Nanosized Si powder (<100 nm) was prepared by pulsed laser deposition. Si/C composite was synthesized by solid-state reaction as following. Firstly, poly(vinyl chloride) (PVC) was dissolved in tetrohydrofuran. Then, nanosized silicon powder and fine graphite powder (~1 μm, Aldrich) were added into the PVC solution with constantly stirring. The solvent was evaporated at 40 °C under stirring to get solid blend. The obtained precursor was then heated to 900 °C for 2 h followed by cooling down to room temperature under mixture atmosphere of Ar (96%) and H_2 (4%). The resulting Si/C composites were ground and sieved by 200-mesh sifter. The composites contain 20 wt% silicon, 30 wt% graphite and 50 wt% pyrolytic carbon. The structure of composites was detected by powder X-ray diffraction measurements (D-max 2550V), and the morphology of powders was inspected by scanning electron microscopy (JSM-6360LV).

2.2. *Electrode fabrication*

The Si/C composite electrodes are constituted by 85 wt% active material, 5 wt% acetylene black and 10 wt% binder on the dry basis. The Si electrodes contain 70 wt% nano-Si, 10 wt% acetylene black and 20 wt% binder. Three binders used in the experiments are polyvinylidene fluoride (PVDF), acrylic adhesive (LA132, Chengdu Indigo Power Sources Co. Ltd, China,) and modified acrylic adhesive (mixture of above acrylic adhesive and sodium carboxyl methyl cellulose (CMC) with 2:1 weight ratio). Firstly, PVDF was dissolved in *n*-methylpyrrolidone (NMP), and the acrylic adhesive and modified acrylic adhesive were dissolved in deionized water, respectively. Then, the active material and acetylene black were homogeneously dispersed in each binder solution by stirring for up to 4 h. The each resulting slurry was cast onto Cu foil, and then dried at 120 °C in vacuum until the solvent was entirely removed.

The adhesion strength between the coating of electrode materials and the Cu current collector was measured by a 180° peeling test. The peeling test was carried out in an omnipotent electronic stress–strain tester (WSM-2KN, Changchun Intelligent Device Co., China). In the tests, the electrodes were cut to a strip of 25 mm width. Then they were fixed to a stainless plate with double faced adhesive tape. The stainless plate was fixed in lower chuck, and Cu foil which was folded 180°, was fixed in the upper chuck. Then the strip was pulled at a speed of 2.0 cm min^{-1}. It was confirmed that de-bonding took place between the coating and the Cu foil in all peeling tests.

The tolerant capability of the binder systems with electrolyte solvent was examined by the swelling test. Solution-cast samples were prepared for swelling tests. For PVDF samples, NMP was used as solvent and subsequently removed under 120 °C in vacuum. PVDF sheets were further hot-pressed under 5 MPa and 120 °C for 30 min. For acrylic adhesive and modified acrylic adhesive, they were dissolved in deionized water and were then cast at 80 °C in vacuum to remove humidity followed by hot pressing at 110 °C and 3 MPa for 30 min. The binder sheets were immerged in the electrolyte solvent (ethylene carbonate plus diethyl carbonate with 1:1 in volume) at either 30 °C or 80 °C. The weight of the sample was measured before swelling and at regular intervals during swelling. The swelling ratio was defined as the weight ratio of the amount of solvent absorbed to the dry weight of sample before swelling.

2.3. *Cell assembly and electrochemical tests*

To evaluate the electrochemical properties of the electrodes, a half-cell containing electrode, Celgard separator, 1 M $LiPF_6$/EC + DMC (ethylene carbonate (EC) plus dimethyl carbonate (DMC) with 1:1 in volume as solvent) electrolyte and lithium foil as counter electrode was assembled in a glove box filled with pure Ar. Cycling tests of the Si/C composite anodes were carried out by Land battery test system at a constant current density of 0.2 mA cm^{-2}, with the cut off potentials being 0.02 V versus Li/Li^+ for discharge and 1.5 V versus Li/Li^+ for charge. For the Si electrodes, a designated discharging capacity of 600 mA h g^{-1} was used for cycling tests. Cyclic voltammograms were recorded at a scan rate of 0.05 mV s^{-1} in the range 0–2.5 V or 0–1.5 V.

3. Results and discussion

It is commonly accepted that the reduction of silicon particle size can improve its electrochemical performance. Therefore, nanosized silicon was used in our experiments. In addition, in order to decrease the porosity and suppress the voltage hysteresis of the composite [21], fine graphite was also added to obtain the Si/C composite. As a mixed-conductor, the pyrolyzed carbon contained in the composite transfers both lithium ion and electron for the active species. Figure 1 shows the X-ray diffraction patterns of nano-silicon, graphite and Si/C composite. Obviously, silicon and

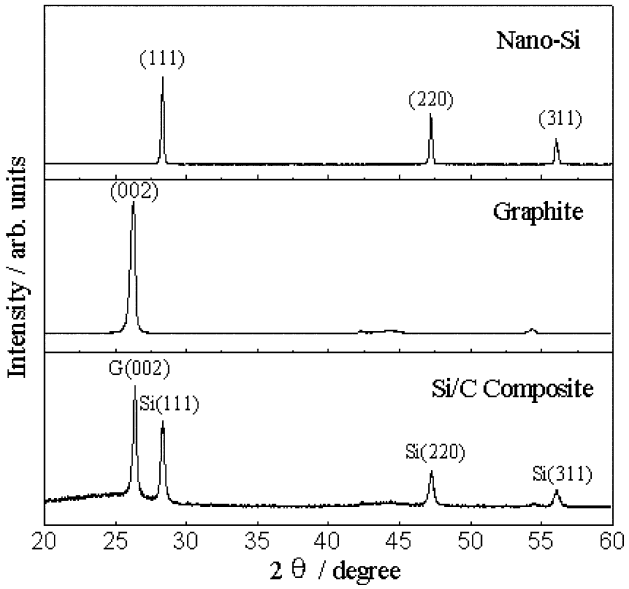

Fig. 1. X-ray diffraction patterns of nano-Si, graphite and Si/C composite.

graphite phases are detected in the Si/C composite. No other phases such as SiC, which is the most possible impurity phase, are detected. This indicates that the composite is a blend of silicon, graphite and pyrolytic carbon. Figure 2 shows a SEM image of the Si/C composite. The particle size of the Si/C composite is about 50 microns, and the particle shape and morphology are irregular due to the grinding process.

Figure 3 compares the cycling performance of Si/C composite electrodes using different binders. Because the first discharging capacity includes the irreversible capacity for forming the solid electrolyte interface (SEI) passivation layer, we discuss the discharging capacity from the second cycle. The PVDF-bound electrode cannot retain stable capacity upon cycling. Only about 67% of the maximum capacity (544 mA h g^{-1}) is maintained after 50 cycles. In contrast, both the

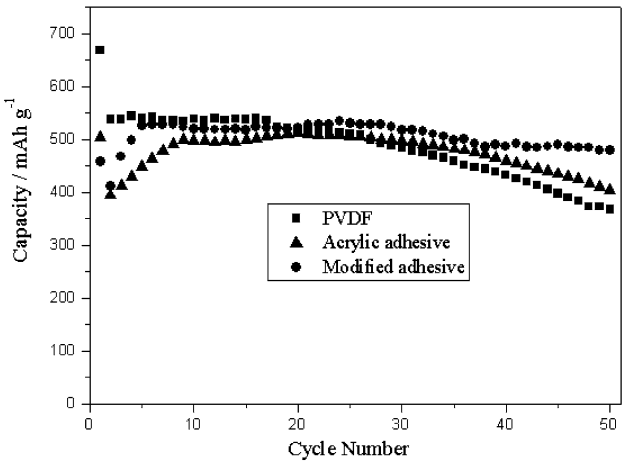

Fig. 3. Cycling performance of Si/C composite electrodes bound by different binders.

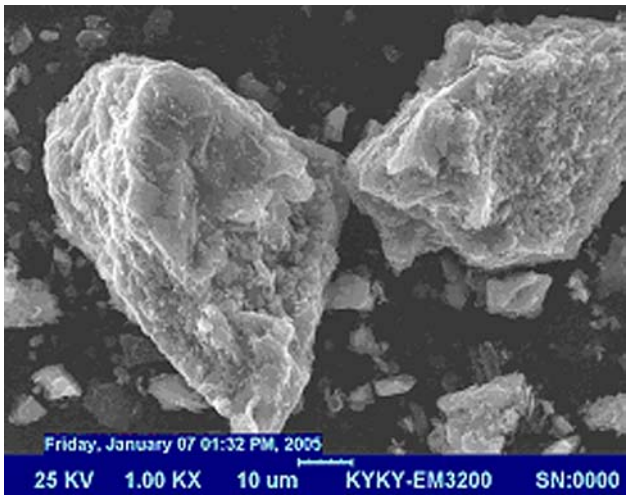

Fig. 2. SEM image of Si/C composite (200 mesh).

electrodes bound by acrylic adhesive and modified acrylic adhesive show better stability in capacity retention upon long cycles. Their capacity retentions are 79% and 90% after 50 cycles, respectively. Apparently, the modified acrylic adhesive greatly improves the cycling performance of the Si/C composite. This suggests that the modified acrylic adhesive is effective in suppressing the morphological deterioration of the Si/C composite upon repeated discharging/charging.

It is also found in Figure 3 that several cycles are required for activating the electrodes to reach its maximum discharging capacity. The cycling times for activating the electrodes vary for different binders. Compared with the PVDF-bound electrode, the electrode bound by acrylic adhesive clearly increases the cycling times for activating the electrode. But the electrode bound by modified acrylic adhesive shows a less activating cycling than the electrode bound by acrylic adhesive. The effect of the binder on the activation of the electrode needs to be investigated in detail.

As discussed above, the improved cycling performance of the Si/C composite is achieved through common effects of the carbon matrix and the novel binder. In order to verify the advantage of the binder, Si electrodes which show much larger volume change than the Si/C composite were used in cycling tests. Figure 4 shows the cycling performance of Si electrodes bound by different binders with a designated discharging capacity of 600 mA h g^{-1}. For the PVDF-bound electrode, the designated capacity only maintains four cycles. In the subsequent cycles, the capacity cannot reach the designated capacity within the cutoff voltage range. In contrast, the electrodes bound by acrylic adhesive and modified acrylic adhesive retain the designed capacity for 13 and 23 cycles, respectively. The enhancement in cycling stability of the Si electrodes by replacing PVDF with acrylic adhesive and modified acrylic adhesive is evident.

Figure 5 presents the cyclic voltammograms of Si/C composite electrodes bound by different binders. For the

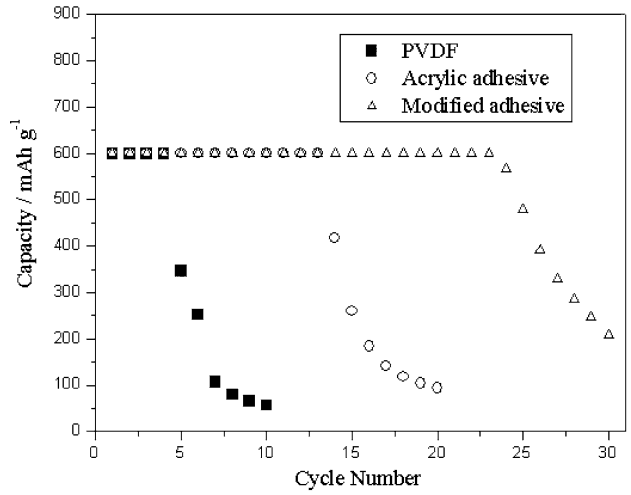

Fig. 4. Cycling performance of Si electrode bound by different binders with a designated discharging capacity of 600 mA h g^{-1}.

electrode bound by PVDF (Figure 5(a)), the cathodic peak at 0.8 V in the first scanning cycle disappears from the second cycle. This may be attributed to the formation of a SEI passivation layer on the electrode surface due to the decomposition of electrolyte. The other cathodic peak near 0 V and two anodic peaks located at 0.2 and 0.5 V, which are stable in the following cycles, correspond to the insertion and extraction of lithium in the Si/C composite. Figure 5(b, c), which show the cyclic voltammograms of the electrodes bound by the acrylic adhesive and modified acrylic adhesive, have essentially the same redox peaks as in Figure 5(a). It is sufficient to say here that the two novel binders are electrochemically stable in the working window and do not cause side reactions.

The adhesion strength of the binder is an important factor for keeping contact between the coating and the current collector, and also between the electrode materials and carbon black. A good cycleability of the electrode requires a strong and elastomeric binder during discharging/charging, especially for electrode materials with larger volume change. To evaluate the adhesion strength between coating and the Cu current collector, 180° peeling test was employed to measure the adhesion strength on a coated strip of 25 mm width. As shown in Figure 6, the peeling strength of the PVDF-bound electrode is 0.40 N and those of the electrodes bound by acrylic adhesive and modified acrylic adhesive

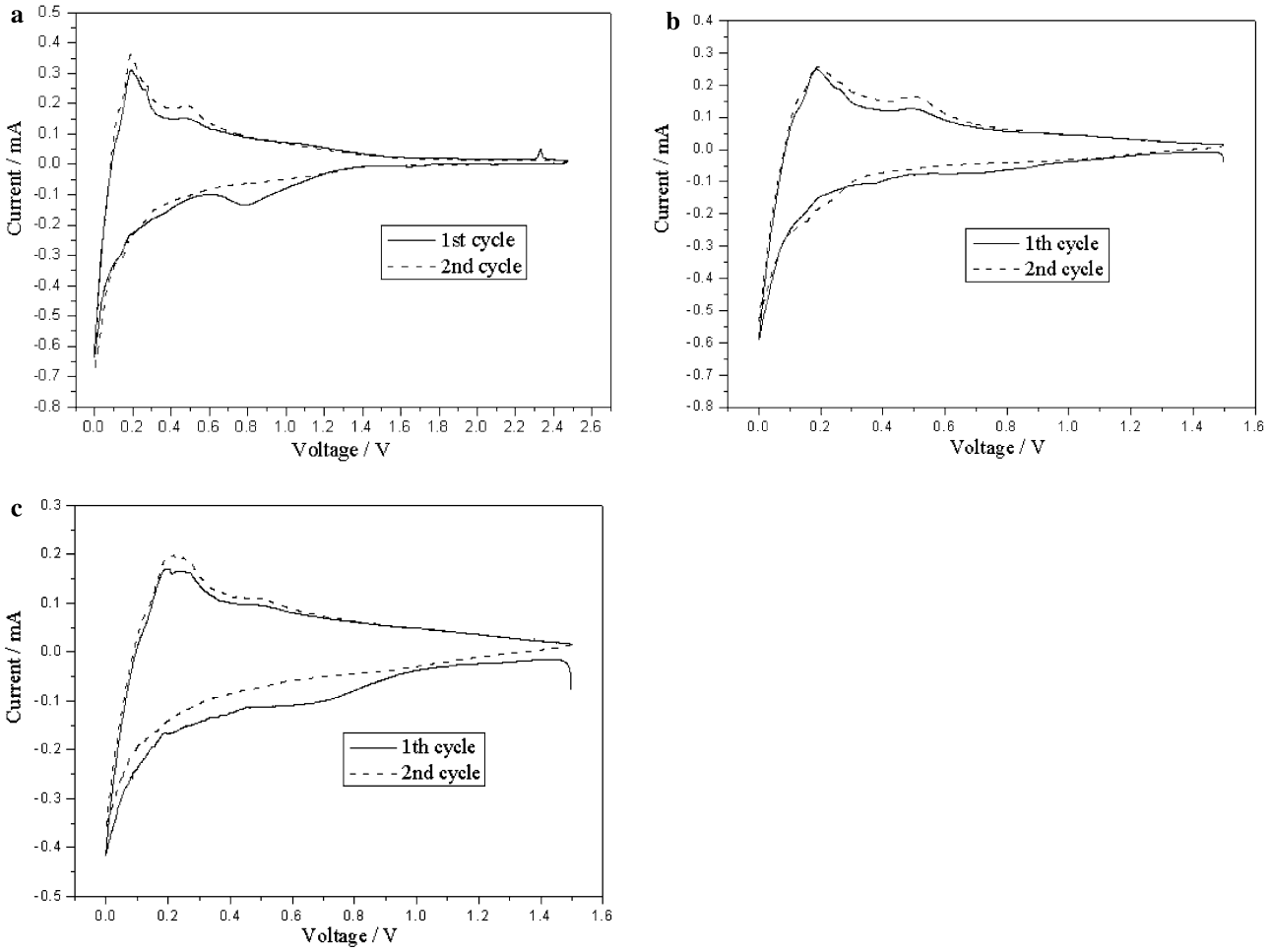

Fig. 5. Cyclic voltammograms of Si/C composite electrodes bound by different binders. (a) PVDF; (b) Acrylic adhesive; (c) Modified acrylic adhesive.

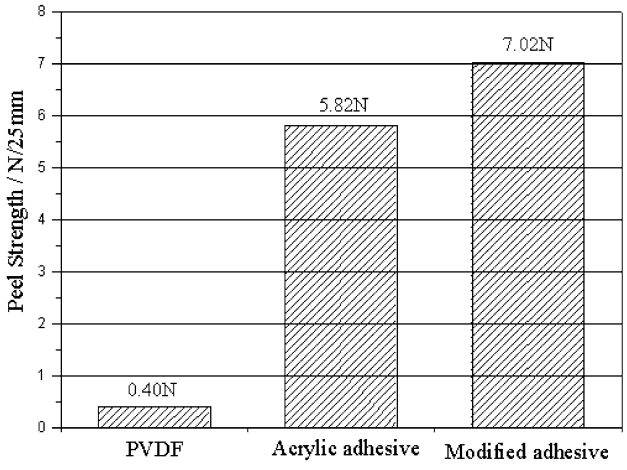

Fig. 6. Comparison of peeling strength of electrodes bound by different binders on 25 mm width strip.

are 5.82 and 7.02 N, respectively. This means that both acrylic adhesive and modified acrylic adhesive can firmly bond the coating on the current collector and thus tolerate a larger extent of volume fluctuation. Furthermore, it is observed that the addition of CMC increases the adhesion strength of acrylic adhesive by 20%. It is well known that CMC is not only an adhesive but also a dispersant. Thus, the addition of CMC to acrylic adhesive prevents particle agglomeration and increases the component distribution uniformity in the coating slurry. Moreover, CMC may improve the wettability of the binder solution with Si/C composite, carbon black and the Cu current collector. Therefore, the Si/C composite and carbon black particles can be contacted well with the binder solution and a firm adhesive bond can be formed. As a result, the addition of CMC enhances the adhesion strength between the coating and the Cu current collector as well as between the Si/C composite and carbon black. All these considerations have advantages of improving cycling performance of Si/C composites bound by modified acrylic adhesive.

Figure 7 shows the relations between swelling ratio and swelling time for PVDF, acrylic adhesive and modified acrylic adhesive sheets in electrolyte solvent at 30 °C and 80 °C. The swelling ratios of three binder sheets reach a stable value after 50 h soakage, indicating that the binders have been saturated with electrolyte solvent. The swelling ratios of PVDF, acrylic adhesive and modified acrylic adhesive sheets are 17, 8 and 15% for 50 h soakage at 30 °C, respectively. Higher temperature speeds up solvent absorption. At 80 °C, PVDF sheet takes up solvent up to 60% of its own weight, while the swelling ratios for acrylic adhesive and modified acrylic adhesive sheets are 35 and 43%, respectively. Furthermore, this figure also shows different swelling rate for three binders. At 80 °C, the absorption of electrolyte solvent becomes saturated within the initial 10 h for PVDF sheet but about 50 h for acrylic adhesive and modified acrylic adhesive sheets. This means that PVDF absorbs solvent much easier than the latter two. It is generally considered that the absorption of solvent may weaken the bonding role of the binder. Therefore, the electrode bound by easy-soaked binder can be easily loosened or even destroyed when the electrode material expands/contracts during lithiation/delithiation. On the other hand, it is also found that the swelling ratio of the binder may be related to electrode activation. The electrode bound by the binder with larger swelling ratio is more easily activated.

4. Conclusion

The cycling performances of the Si/C composite electrode and Si electrode are enhanced by replacing PVDF with acrylic adhesive and modified acrylic adhesive as binder. The capacity retention after 50 cycles increases from 67% for PVDF-bound electrodes to 79 and 90% for electrodes bound by acrylic adhesive and modified acrylic adhesive, respectively. Both acrylic adhesive and

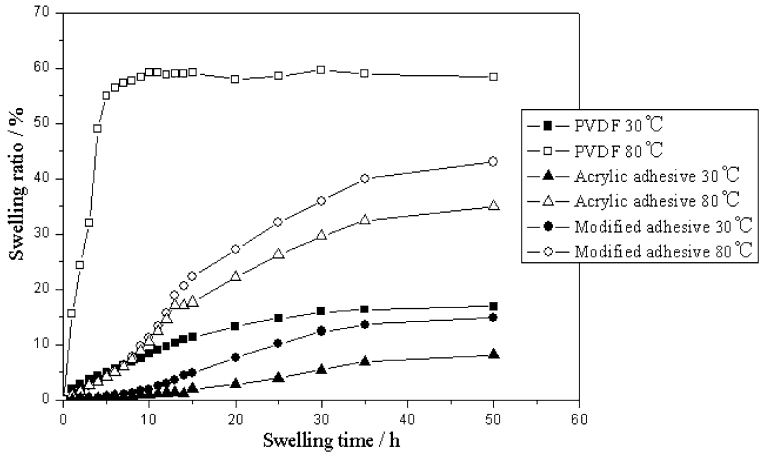

Fig. 7. Swelling ratio versus swelling time in electrolyte solvent (EC:DMC with 1:1 in volume) for PVDF, acrylic adhesive and modified acrylic adhesive sheets at 30 °C and 80 °C.

modified acrylic adhesive are electrochemically stable in the organic electrolyte. These two novel binders exhibit larger adhesive strength and smaller solvent absorption than PVDF. It is believed that these binders would also be suitable for use in other electrode materials with large volume change.

Acknowledgements

This research was supported by National High-Tech Research and Development Program of China.

References

1. M. Yoshio, H.Y. Wang, K. Fukuda, Y. Hara and Y. Adachi, *J. Electrochem. Soc.* **147** (2000) 1245.
2. H.Y. Lee and S.M. Lee, *J. Power Sources* **112** (2002) 649.
3. T. Hasegawa, S.R. Mukai, Y. Shirato and H. Tamon, *Carbon* **42** (2004) 2573.
4. J.H. Ryu, J.W. Kim, Y.E. Sung and S.M. Oh, *Electrochem. Solid-State Lett.* **7** (2004) A306.
5. H. Li, X.J. Huang, L.Q. Chen, Z.G. Wu and Y. Liang, *Electrochem. Solid-State Lett.* **2** (1999) 547.
6. H. Jung, M. Park, Y.G. Yoon, G.B. Kim and S.K. Joo, *J. Power Sources* **115** (2005) 346.
7. G.X. Wang, J.H. Ahn, J. Yao, S. Bewlay and H.K. Liu, *Electrochem. Commun.* **6** (2004) 689.
8. Y. Liu, K. Hanai, J. Yang, N. Imanishi, A. Hirano and Y. Takeda, *Solid State Ionics* **168** (2004) 61.
9. J. Yang, B.F. Wang, K. Wang, Y. Liu, J.Y. Xie and Z.S. Wen, *Electrochem. Solid-State Lett.* **6** (2003) A154.
10. S.M. Hwang, H.Y. Lee, S.W. Jang, S.M. Lee, S.J. Lee, H.K. Baik and J.Y. Lee, *Electrochem. Solid-State Lett.* **4** (2001) A97.
11. II. Kim, G.E. Blomgren and P.N. Kumta, *Electrochem. Solid-State Lett.* **6** (2003) A157.
12. G.A. Roberts, E.J. Cairns and J.A. Reimer, *J. Power Sources* **110** (2002) 424.
13. G.X. Wang, L. Sun, D.H. Bradhurst, S. Zhong, S.X. Dou and H.K. Liu, *J. Power Sources* **88** (2000) 278.
14. S. Ohara, J. Suzuki, K. Sekine and T. Takamura, *J. Power Sources* **136** (2004) 303.
15. T.D. Hatchard and J.R. Dahn, *J. Electrochem. Soc.* **151** (2004) A1628.
16. J.B. Kim, H.Y. Lee, K.S. Lee, S.H. Lim and S.M. Lee, *Electrochem. Commun.* **5** (2003) 544.
17. Z.H. Chen, L. Christensen and J.R. Dahn, *Electrochem. Commun.* **5** (2003) 919.
18. W.R. Liu, M.H. Yang, H.C. Wu, S.M. Chiao and N.L. Wu, *Electrochem. Solid-State Lett.* **8** (2005) A100.
19. B.F. Wang, J. Yang, J.Y. Xie, K. Wang and Z.S. Wen, *J. Ceram. Soc. Jpn.* **112**(Supplement 112–1) (2004) S649.
20. Y. Liu, K. Hanai, T. Matsumura, N. Imanishi, A. Hirano and Y. Takeda, *Electrochem. Solid-State Lett.* **7** (2004) A492.
21. Z.S. Wen, J. Yang, B.F. Wang, K. Wang and Y. Liu, *Electrochem. Commun.* **5** (2003) 165.